Vol 13 No 5, May 2004
1009-1963/2004/13(05)/0720-05

Chinese Physics

© 2004 Chin. Phys. Soc.
and IOP Publishing Ltd

Synchrotron small angle x-ray scattering study of dye-sensitized/-unsensitized TiO_2 nanoparticle colloidal solution*

Hong Xin-Guo(洪新国)[a)†], Du Lu-Chao(都鲁超)[b)],
Ye Man-Ping(叶满萍)[b)], and Weng Yu-Xiang(翁羽翔)[b)]

[a)] *Institute of High Energy Physics, Chinese Academy of Sciences, Beijing* 100039, *China*

[b)] *Institute of Physics, Chinese Academy of Sciences, Beijing* 100080, *China*

(Received 28 August 2003; revised manuscript received 19 November 2003)

The wide-gap semiconductor TiO_2 nanoparticles with and without dye sensitization have been studied by small angle x-ray scattering using synchrotron radiation. Surface properties of the colloidal TiO_2 nanoparticles have been analysed in terms of the surface fractal dimensions (D_s), showing that D_s changes from 3.25 to 2.34 when TiO_2 nanoparticles are sensitized by ATRA (all-trans-retinoic acid), which reveals that the surface of the particles become relatively smooth after dye sensitization. The size distribution of gyration radius of TiO_2 nanoparticles in the colloids $M(R_g)$ has been successfully determined by the Shull–Roess method. The main peak of $M(R_g)$ for the unsensitized TiO_2 colloid is located at 2.1nm, corresponding to a spherical diameter of 5.4nm, and this value for the ATRA sensitized TiO_2 increases to 2.4nm, indicating a spherical diameter of 6.4nm. Such a size enlargement of TiO_2 nanoparticles suggests that there is a coating of ATRA on the TiO_2 surface, supporting the view that a monolayer of the dye has been attached to the surface of the TiO_2 nanoparticle.

Keywords: TiO_2 nano-particles, small angle x-ray scattering, colloid, solar cell
PACC: 6110, 2920, 8270, 6146, 8270D

1. Introduction

The physical properties of nanoscale particles (diameter 1–50nm) are significantly different from those of microscopic (1–500 μm) or readily crystallizing materials of identical chemical composition.[1–5] Among the various kinds of nanocrystalline materials, wide-gap semiconductor titanium dioxide has been well known for its various applications including photovoltaic, electrochromic, photochromic, electroluminescence, photocatalysis nanoelectronic devices and sensors.[6,7]

In many applications, the assembling of dye molecules is involved on the TiO_2 nanoparticulate surface. To achieve the expected effect, the dye-assembling should be carefully engineered. The successful engineering of dye molecules on TiO_2 nanoparticles is the invention of the dye-sensitized TiO_2 nanoparticle solar cell, known as the Grätzel cell, which has the advantages of high efficiency and low cost.[8,9] TiO_2 was used in the form of nanocrystalline layers, in combination with organic electrolytes (acetonitrile and ethylene carbonate) and ruthenium complexes as sensitizers. An important requirement was the attachment of the ruthenium complex to the TiO_2 surface by carboxylic groups.[10] It is known that the dye could function most efficiently if it is chemisorbed on the surface of a semiconductor.[11,12] Such kind of dye-sensitized cells differ from the conventional semiconductor devices in that they separate the function of light absorption from that of charge carrier transport. The device is based on TiO_2 particles of around ten nanometres in size, coated with a monolayer of charge-transfer dye to sensitize the film for light harvesting.[8] Therefore, it is obvious that the size distribution of TiO_2 nanoparticles and the interfacial character are important in the molecular engineering at the interface.[9,13,14] Two kinds of structural

*Project supported by the National Natural Science Foundation of China (Grant No 10375075) and by the Innovation Foundation of the Institute of High Energy Physics, Chinese Academy of Sciences.

†To whom correspondence should be addressed. Tel: 86-10-88235993, FAX: 86-10-88236229 E-mail: hongxg@ihep.ac.cn

information, i.e. the size and surface properties, are essential for such a purpose. The size effect and surface properties of semiconductor nanoparticles have been the subject of intense research interest in recent years.[15–17]

Solution x-ray scattering [18] using synchrotron radiation x-rays has proven to be a very useful technique for obtaining structural details such as the size distribution and surface properties of the nanoparticles. The low-resolution shape and fractal dimension of TiO_2 in the solution allows a more detailed study on the nanoparticle and its chemisorption. In our previous work, ATRA sensitized TiO_2 colloidal solution has been studied by nanosecond and femtosecond time-resolved difference absorbance spectroscopy for its interfacial electron transfer process, and it has also been discovered that ATRA can serve as a transient molecular probe to different kinds of surface binding between the surface titanium atoms, as well as the polarity of the medium.[19] We have also noticed that this molecular probe indicates the polarity of the micro-environment of the probe molecule rather than that of the bulk medium. Therefore it is imperative to understand the arrangement of the ATRA molecule on the TiO_2 surface. In this paper, we present the results of small-angle x-ray scattering (SAXS) study on ATRA-sensitized/unsensitized TiO_2 colloidal solutions, which support the view that the ATRA molecules form a monolayer on the TiO_2 surface with carboxylic groups binding on the TiO_2 surface and the hydrophobic moiety pointing towards the medium. To our best knowledge, this is the first direct evidence for the presence of dye molecule layer coated on the TiO_2 nanoparticle in the solution.

2. Experiment

The SAXS experiments were carried out on beamline 4B9A at the Beijing Synchrotron Radiation Facility (BSRF), using a home-made SAXS apparatus. The x-rays from a bending magnet were focused in both horizontal and vertical directions by a Pt-coated toroidal mirror, then monochromatized by a double Si(111) crystal monochromator with a fixed exit. The energy range of the beamline was from 3 to 12keV with a resolution of 3×10^{-4}.[20] The storage ring was operated at 2.2GeV with a current around 80mA during the measurements. The wavelength of the incident monochromatic x-ray beam used in the experiment was 0.154nm. The scattered x-ray intensities were recorded using an image plate technology, as a function of the modulus of the scattering vector, $h = 4\pi\sin\theta/\lambda$, where 2θ is the scattering angle. The detector for SAXS data collection was the image plate (IP) system Fuji BAS-2500, with an active area of 400mm by 200mm and a minimum pixel size of 50μm.

The sample-to-detector distance of 1553.0mm and the x-ray wavelength of λ=0.154nm allow a coverage of scattering vector interval of $0.1 < h < 2.5\text{nm}^{-1}$. The background scattering, such as parasitic scattering intensity and those produced by air and slits, was subtracted from the total measured SAXS intensity. The absorption of the samples was corrected. SAXS analysis was conducted in terms of several programs coded by using Visual-Fortran.

The samples were encapsulated inside a cell between two thin parallel diamond windows. Data acquisition time was typically 5–20min, depending on the scattering intensity. TiO_2 nanoparticle was prepared by hydrolysis of Ti(IV) (iso-propoxide)$_4$ under acidic condition.[21] The concentration of TiO_2 in water was 2.0g/L. All-trans-retinoic acid (Aldrich), titanium(IV) 2-propoxide (Alfa, 98%) and 8-Apo-8'carotenal (Aldrich) were used without further purification. The ATRA sensitized TiO_2 colloidal solutions were subjected to high purity N_2 gas bubbling for at least half an hour to remove the dissolved oxygen.[22] Powdered TiO_2 sample was prepared by room temperature rotary evaporation of the solvents for x-ray diffraction measurement.

3. Results and discussion

Figure 1 shows the scattering intensity recorded by an image plate for 0.33g/L TiO_2 in water at the BL4B9A beamline of BSRF. The centre of the beam can be fixed by interpolating from the lower side toward higher side at first and then choosing the middle of the interpolating line. Averaging several such middle points, as shown in the figure, gives the position of beam centre with excellent accuracy. The inset of Fig.1 shows the derived scattering intensity as a function of the modulus of scattering vector h.

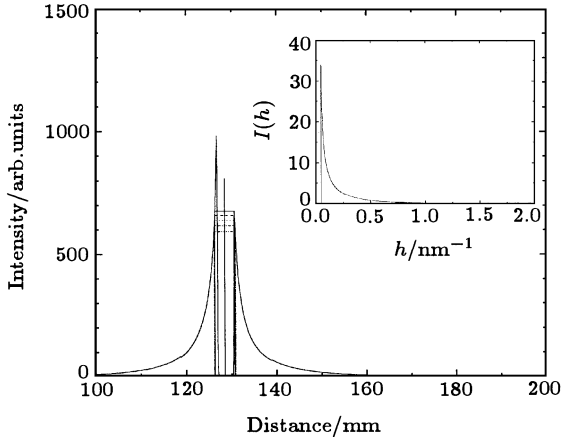


Fig.1. Small-angle x-ray scattering curves of the TiO_2 samples in aqueous solution.

The average radius of gyration of nanoparticles in solution can be calculated by [23]

$$I(h) = I_e N n^2 \exp[-h^2 R_g^2/3], \quad (1)$$

where I_e is the scattering intensity per electron, N is the number of the scatterers, and n is the number of electrons. In practice, a linearized representation will be used, by plotting $\ln[I(h)]$ vs h^2 (Guinier plot). However, the Guinier radius cannot be calculated from the appropriate plot of the scattering data, i.e. a straight line was not observed in the initial section of the logarithmic intensity versus h^2 plot, as shown in Fig.2. This deviation is due to the polydisperse size distribution of the structural units in the solution. As shown in the small angle region of Fig.2, the absolute value of the slope of TiO_2 with ATRA is larger than that in water, implying a different size distribution in these colloids.

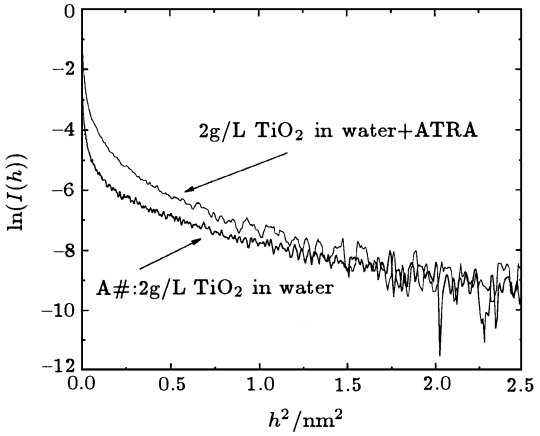


Fig.2. Guinier plot of the SAXS data for the samples; (a) 2g/L TiO_2 in water, (b) 2g/L TiO_2 in water+ATRA.

The concepts of fractal geometry can be applied successfully to the study of solid surfaces. Traditionally, the fractal dimension D is calculated from adsorption measurements, however the SAXS gives an excellent possibility to observe the fractal behaviour of the systems.[24–26] The surface fractal dimension D_s is defined as the degree of surface roughness or irregularity which falls in the range $2 \leq D_s \leq 3$. For a perfectly smooth surface D_s=2, referring to the dimension of a Euclidean surface; while for a highly rough, very irregular one, D_s has a value of 3. The surface fractal dimensions D_s can be computed from the scattering data using the following equation:

$$D_s = 6 - |\text{slope}_2|, \quad (2)$$

where $|\text{slope}_2|$ is the slope of the log I vs log h scattering curves, and slope_2 is determined in the Porod regime of the scattering variable.

Figure 3 shows the results. It is found that D_s=3.25±0.1, 2.34±0.1 for the 2g/L TiO_2 in water and that with ATRA dye respectively, both of which deviate from 2. The value of D_s in water suggests that the particle has a rough surface. However, it is worthy to note that the particle in ATRA solution has a quite smooth surface, indicating a distinct combination of TiO_2 and ATRA dye molecules. This view is supported by the corresponding size distribution, as shown in Fig.5.

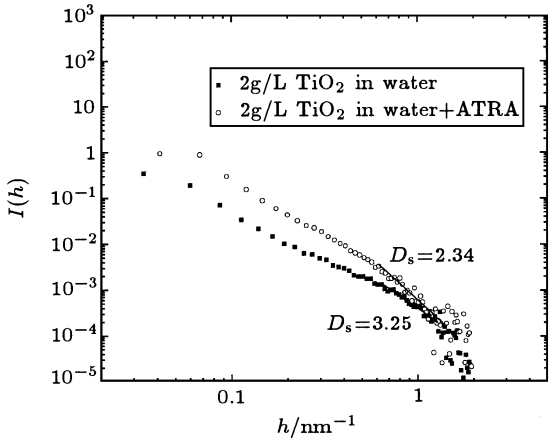


Fig.3. log$I$-log$h$ representations of the SAXS data.

The Guinier approximation (Eq.1) is valid for monodispersive spherical particles, but it can be extended to any anisotropic shape.[23,27] If the assumption is observed, the log I vs h^2 plot is linear. According to Fig.2, none of the samples show a straight line in the initial section of this plot: that is, the size

of the scattering particles cannot be described by the Guinier radius. The deviation from the Guinier plot is because of the polydispersive size distribution of the scattering particles. Further detailed information can be obtained by the method of Shull and Roess [28] which described the scattering curves in the Guinier range by employing various types of size distribution functions. If a Maxwellian type of distribution is assumed, the scattering curve can be transformed into a straight line by a fitted shift $(3/r_0^2)$ according to the equation

$$\log I = c_2 - \frac{(n+4)}{2}\log(h^2 + 3/r_0^2), \qquad (3)$$

where c_2 is a constant, and n and r_0 are the parameters of the Maxwellian distribution function in the following equation:

$$M(R_g) = \frac{2}{r_0^{n+1}\Gamma((n+1)/2)} r^n \exp(-R_g^2/r_0^2). \qquad (4)$$

$M(R_g)$ is normalized to the total mass of the scattering particles. Figure 4 shows the linearization of the $\log I$ vs $\log h^2$ representation of the intensity curves for the 2g/L TiO_2 in water and that sensitized with ATRA dye.

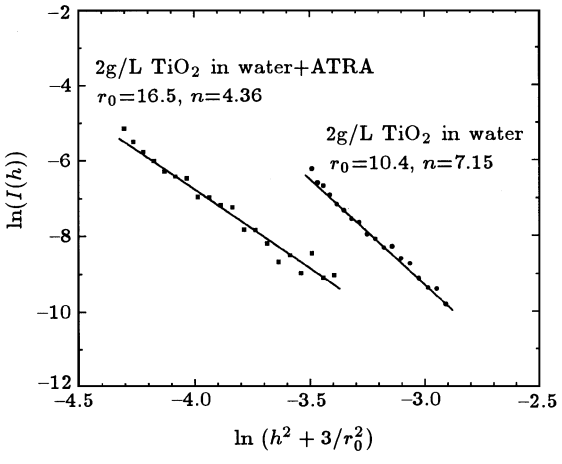


Fig.4. The linearized $\log I - \log(h^2 + 3/r_0^2)$ representations of the SAXS.

A Maxwellian type distribution can be obtained by using the method of Shull and Roess, and the obtained distributions of Guinier radius are shown in Fig.5. The similarity of the size distribution curves suggests no significant differences in the matrix structure. Further assuming that the particles are spherical, the characteristic diameters calculated, $2R = 2(5/3)^{1/2}R_g$, are about 5.4nm for the sample of 2g/L TiO_2. The XRD measurement of powdered TiO_2 shows that the average size of TiO_2 nanoparticles is 5.9nm based on Sherrer's formula. Obviously, these two different methods lead to a consistent value of the average size. It should be noted that the $M(R_g)$ peak position for the ATRA sensitized TiO_2 colloidal solution has a value of 2.4nm, corresponding to a spherical diameter of 6.4nm, i.e. the diameter increases by about 1nm when ATRA is added to the colloidal solution. Since the maximally extended length of an ATRA molecule is 1.56nm, which is an extended polyene structure, and the real length can be shorter than this value, it is natural to conclude that our result supports the view that a monolayer of the ATRA molecules has been attached to the surface of TiO_2 nanoparticle via the carboxylic group, with the extended retinyl moiety pointing out towards the solvent.

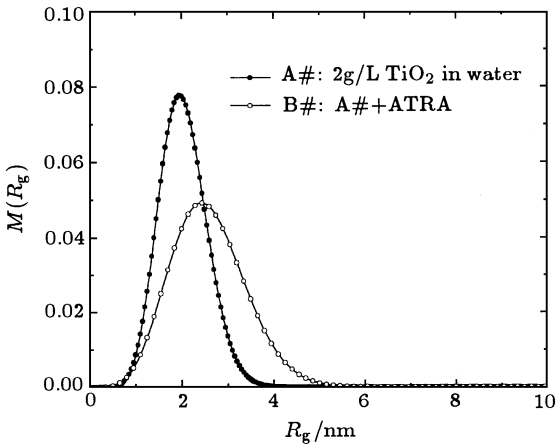


Fig.5. Guinier radius distribution calculated from the SAXS curves using a Maxwellian type distribution.

4. Conclusions

We have performed a SAXS measurement on the wide-gap semiconductor TiO_2 nanoparticles in colloidal solution using synchrotron radiation. The surface properties of the TiO_2 nanoparticles in aqueous solutions with and without ATRA dye have been analysed in terms of surface fractal dimensions. The size distribution of gyration radius of TiO_2 nanoparticles in these solutions $M(R_g)$ has been successfully determined by the Shull–Roess method. The main peak of $M(R_g)$, which is located at 2.1nm, corresponding to a spherical diameter of 5.4nm for the aqueous solution, increases to 2.4nm, i.e. corresponding to a spherical diameter of 6.4nm for the colloidal solution with ATRA dye. This enlargement in the size of TiO_2 nanoparticle indicates that there is a distinct combination of TiO_2 and ATRA dye molecules, supporting

the view that a monolayer of the dye molecules has been attached to the surface of the TiO_2 nanoparticle. These results provide direct evidence for the layered dye coating on the TiO_2 nanoparticle in the solution phase.

Acknowledgment

We would like to thank Professor Z. H. Mai and Professor T. D. Hu for their support of this research. Assistance in the experiment from Professor B. Z. Dong, Dr. Z.H. Wu and Z. J. Chen is gratefully acknowledged.

References

[1] Enea O and Bard A J 1986 *J. Phys. Chem.* **90** 301
[2] Lianos P and Thomas J H 1986 *Phys. Lett.* **125/3** 299
[3] Kortan A R, Hull R, Opila R L, Bawendi M G, Steigerwald M J, Carrol P J and Brus L E 1990 *J. Am. Chem. Soc.* **112** 1327
[4] Resch G, Eychmüller A, Haase H and Weller H 1992 *Langmuir* **8** 2215
[5] Chemseddine A and Weller H 1993 *Ber. Bunsenges. Phys. Chem.* **97** 636
[6] Brinker C J and Scherrer G W 1990 *Sol Gel Science the Physics and Chemistry of Sol-Gel Processing* (San Diego, CA: Academic)
[7] Gerfin T, Gratzel M and Walder L 1997 *Charge-Separating and Charge-Injecting Devices* **44** (New York: Wiley)
[8] O'Regan B and Grätzel M 1991 *Nature* **353** 737
[9] Hagfeldt A and Grätzel M 2000 *Acc. Chem. Res.* **33** 269
[10] Anderson S, Constable E C, Dare-Edwards M P, Goodenough J B, Hamnet A, Seddon K R and Wright R D 1979 *Nature* **280** 571
[11] Dare-Edwards M P, Goodenough J B, Andrew A, Seddon K R and Wright R D 1981 *Faraday Discuss.* **70** 285
[12] Tsubomura H, Matsumura M, Noyamura Y, Amamyiya T 1976 *Nature* **261** 402.
[13] Bach U, Lupo D, Comte P, Moser J E, Weissörtel F, Salbeck J, Spreitzer H and Grätzel M 1998 *Nature* **395** 583
[14] Kubo W, Murakoshi K, Kitamura T, Wada Y, Hanabusa K, Shirai H and Yanagida S 1998 *Chem. Lett.* 1241
[15] Miller R J D, McLendon G L, Nozik A J, Schmickler W and Willig F 1995 *Surface Electron-Transfer Processes* (New York: VCH)
[16] Kamat P V and Meisel D 1997 *Semiconductor Nanoclusters—Physical, Chemical, and Catalytic Aspects* (Amsterdam: Elsevier) Vol.103
[17] Nozik A J and Memming R 1996 *J. Phys. Chem.* **100** 13061
[18] Svergun D I and Stuhrmann H B 1991 *Acta Crystallogr.* A **47** 736
[19] Weng Y X, Li L, Liu Y, Wang L and Yang G Z 2003 *J. Phys. Chem.* B **107** 4356
[20] Dong B Z, Sheng WJ, Yang H L and Zhang Z J 1997 *J. Appl. Crystallogr.* **30** 877
[21] Wang Z S 2001 Study on the photo-electron chemical properties of dye-sensitized TiO_2 nanocrystalline solar cell *Ph.D. Thesis* College of Chemistry and Molecular Engineering, Peking University, China
[22] Weng Y X, Li Long, Liu Y, Wang L, Yang G Z and Sheng J Q 2002 *Chem. Phys. Lett.* **355** 294
[23] Guinier A and Fournet G. 1955 *Small-angle scattering of x-rays* (London: Wiley)
[24] Avnir D and Farin D 1989 *The Fractal Approach to Heterogeneous Chemistry* Ed D Avnir (New York: Wiley) Chapter 4
[25] Reich M H, Russo S P, Snook I K and Wagenfeld H K 1990 *J. Colloid Interface Sci.* **135** 353
[26] Snook I K and McMahon P 1993 *Langmuir* **9** 2726
[27] Kakudo M and Kasai N 1992 *x-ray Diffraction by Polymers* (Tokyo: Kodashe)
[28] Shull C G and Roess L C 1947 *J. Appl. Phys.* **18** 295